

Spectroscopic techniques as a diagnostic tool for early detection of osteoporosis[†]Kanika Singh¹, Kwang-Sung Lee¹, Donggeun Lee^{1,*}, Yong Ki Kim² and Kyung Chun Kim^{1,*}¹School of Mechanical Engineering, Pusan National University, Busan 609-735, Korea²Endocrinology and Metabolism, College of Medicine, Pusan National University, Busan 602-739, Korea

(Manuscript Received December 23, 2009; Revised May 6, 2010; Accepted May 20, 2010)

Abstract

Osteoporosis (OP) a kind of bone disease, is very serious in particular for old persons, and may lead them to immobility and death. Early detection of the diseases is the first consideration for the patients to have more options to live a healthy life. The biomarkers or bonemarkers provide a promising challenge in clinical proteomics for early disease detection. In this paper, optical techniques such as Fourier Transform Infrared Spectroscopy (FTIR) and UV/Visible spectroscopy are employed to find the bone markers and emphasis has been given on noninvasive modalities for early detection of osteoporosis. Blood plasma samples procured from two groups, patients and healthy persons were tested. Both of the optical techniques revealed obvious differences in the spectra; between two groups, for example, increase in intensity for OP persons. New peaks were found at 1646, 1540, 1456 and 1077 cm⁻¹ in FTIR spectra. Except 1588 cm⁻¹, we showed decrease in spectral intensity of OP persons. In UV/Visible spectroscopy results, new peaks appeared in the OP patients spectra at the wavelength of 279 nm and 414 nm. These differences in the spectra of the two types samples, allow rapid and cost-effective discrimination of the potential patients with the optical techniques which were verified by the bone densitometer in the hospitals. The new and novel technique is quick, reliable and effective.

Keywords: Bone densitometry; Bonemarkers; Optical detection; Osteoporosis

1. Introduction

Osteoporosis (OP), a serious bone disease, silently creeps itself has no specific symptoms; its main consequence is the increased risk of bone fractures. When the unaware patient realizes the seriousness of the disease, the diagnosis and treatments becomes unaffordable. In addition, the OP causes degradation in the bone condition especially of old persons because of increasing skeletal fragility with aging and possibly leads them to death. The medication given at right time can control the OP only if detected at the early stage [1-4]. The OP is still considered to be under-diagnosed and under-treated, hence challenges lie in identifying and understanding the totality of features and characteristics.

The degrading the bone conditions in the OP [2-4] is primarily due to excessive demineralization of bone, bone mineral density (BMD) has been thought as a basis for the diagnosis of the OP and typically measured by a dual-energy X-ray Absorptiometry (DXA) in the hospitals. However, this technique has several disadvantages e.g. radiation effects, no early detection, invasive but time-consuming and unaffordable

measurement [3, 4]. Hence, urgent need for easy, rapid and cost-effective tools for early detection and home care of the OP just like diabetes are required. More basically, discovery of distinct biomarkers between healthy and patients groups, if possible, would be the first step to get an insight of the mechanism for generation and progress of the OP as well as development of more efficient medications.

These days, different diseases are diagnosed by using biochemical or pathological analysis. Blood analysis is mostly used for the diagnosis of the diseases. Biomarker giving the evidence of the disease is a bio-molecule or protein which can be identified in the blood plasma. For example, these biomarkers are well established for the early detection of cancer [1]. Likewise, as bone metabolism is responsible for the bone condition [4-7], such biomarkers from blood analysis can be another kind of bonemarkers for predicting of the OP and bone fractures. Unfortunately, conventional blood analysis is mostly complicated, tedious and time consuming. Thus one seeks other ways to replace this blood analysis. It is notable that optical [8-17] and/or electrical techniques are in common use for the detection of proteins, which are simple to be used to give quick results for the detection of various diseases, like bone mineral density [12, 13], leukemia [17], cardiovascular diseases in blood plasma [10].

Here, we therefore attempted, for the first time, to find the

[†]This paper was recommended for publication in revised form by Associate Editor Yong Tae Kim

*Corresponding author. Tel.: +82 51 510 2365, Fax.: +82 51 512 5236

E-mail address: donglee@email.ac.kr; kckim@pusan.ac.kr

© KSME & Springer 2010

bonemarkers indicating the potential patients of the OP by employing two optical techniques such as FTIR and UV/Visible spectroscopy. The two techniques are both powerful analytical tools for determining the microscale molecular composition of a variety of cells [9] and have importance in a study of biological structures and conformation of molecules, like proteins, lipids, acids, and so on. Blood plasma samples procured from two groups of patients and healthy persons were tested. Both of the optical techniques revealed obvious differences in the spectra between two groups, for example, increase in intensity for OP persons. Also, classifications are performed on all investigated group members in the vicinity of each of several spectral peaks. The both groups are revealed to have a clear heterogeneity within all investigated applicants. These differences in the spectra between the two groups were confirmed to be fairly consistent with those in T scores from the BMD measurements.

2. Material & Method

2.1 Blood sampling

Blood samples were procured from Pusan National University Medical Hospital, Busan, South Korea. Approximately 3 ml of venous blood was obtained from the arms of two research groups consisting of 5 healthy persons and 5 patients suffered from osteoporosis. Blood samples are taken from each person at five different times with two-day intervals. In addition, the samples are taken exactly at 9 am to avoid unnecessary diurnal variation of the persons. All group members were males and females between the age group of 30 and 75 years. The blood samples were freshly centrifuged for 10 min at 3,500 rpm in a centrifuge (KUBOTA co., JP, KUBOTA 20101) so that the plasma was separated from the cellular material. The plasma was then stored at -20 °C for further optical measurements.

2.2 Sample preparation for optical measurement

Since ordinary glass slide exhibits strong absorption in the wavelength range of interest for the present FTIR measurement, zinc selenide (ZnSe) crystals (3 mm-diameter thin disc) which is highly transparent to IR radiation in a wavelength range of 0.5 to 20 micron, was used for the measurements. A drop of 1 microliter of the plasma sample taken by a micropipette (Pipetman Gilson X53095B) was placed on a certain area on the ZnSe crystal and air-dried for 30 min at room temperature, and then examined by the FTIR microspectroscope (Thermo-Electron co., USA, Nicolet 380). All tubular containers of the plasma samples were well sealed to prevent contamination of the samples.

The blood plasmas of the healthy and patient samples were diluted with DI water to 1 % by weight for the measurement of UV/Visible spectroscopy (Varian co., USA, Cary 5E). Two 25 mm-long 50 mm-wide cuvettes containing the samples were placed in the UV/Visible spectrometer. Then spectral

absorptivity of the sample was scanned in a range of wavelength from 250 to 500 nm.

2.3 Optical techniques

The demineralization initiated by poor nutrition and hormone changes can generate an imbalance in bone metabolism activities, resulting in a release of trace level concentration of some proteins into the blood plasma, especially at the beginning of the progressing disease, as expected from the ELISA (Enzyme linked immune-absorbent assay) testing [8]. Also the optical techniques employed in this study can analyze the microliter of the plasma with no reagents as well as no damage to the samples [10-12]. Therefore, FTIR [14-20] and UV/Visible spectroscopy [21] are first used to differentiate patients with healthy persons and further the bone density measurements are performed for the same groups to verify the results.

2.3.1 Fourier Transform Infra-Red spectroscopy measurement

FTIR spectroscopy uses a Michelson interferometer and the signal is recorded as a function of the optical path difference between the fixed and the movable mirror using a beam-splitter. This interferogram or the spectral signal is calculated as a function of wavelength by applying a Fourier Transform (FT). The advantage of this technique is the higher spectral resolution and a typically higher throughput in intensity [14]. The FTIR [14-26] has been therefore implemented to detect minute changes in concentration or modification of the surface groups of proteins in human plasma.

The FTIR spectra are recorded in the wave number range of 600-4000 cm^{-1} with a precision better than 0.1 cm^{-1} by a FTIR spectrometer (Thermo-Electron co., Nicolet 380) equipped with a KBr beamsplitter and a DTGS (Deuterated TriGlycine Sulfate) detector that is highly sensitive to the mid-IR range. Thirty two scans are continuously performed for an individual sample at a resolution of 4 cm^{-1} and then averaged to give a spectrum for the sample. Such measurements are repeated five times for different samples taken from a person. The five FTIR spectra are again averaged and presented as single line. The baseline of each spectrum is corrected using OMNIC software supplied by the manufacturer. The Peak-Fit software program by SSPS is used for analysis of the spectrum.

2.3.2 UV/Visible spectroscopy measurement

UV/Visible spectroscopy has been routinely used in a quantitative determination of an unknown compound dissolved or suspended in a liquid, typically in terms of its concentration using the Beer Lambert Law. The present UV/Visible spectrometer (Varian co., USA, Cary 5E) employing two radiation sources such as deuterium and tungsten lamps covers a wide range of wavelength from 190 nm to 1100 nm. Once the incident light passes through the plasma sample, the transmitted light is passed through a spectrograph source lens, a small aperture which limits the size of the incoming beam and pre-

Table 1. T-score criteria for the diagnosis of the osteoporosis, J.A. Kanis et al., J. Bone Miner. Res. 9, 1137-1141 (1994).

Status	T-score
Normal	+2.5 to -1.0, inclusive
Osteopenia	Between -1.0 and -2.5
Osteoporosis	≤ -2.5
Severe osteoporosis	≤ -2.5 + fragility fracture

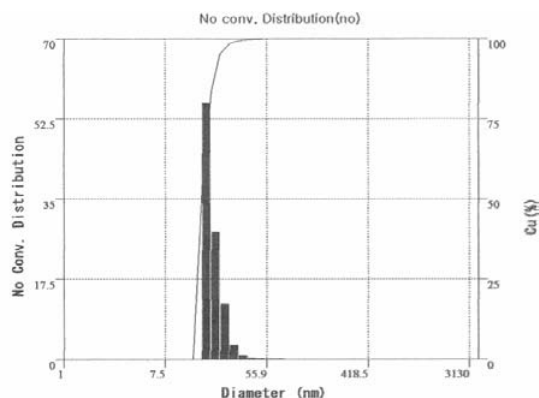


Fig. 1. Hydrodynamic size distribution of blood plasma cells using dynamic light scattering. The left vertical axis is the number of conversion distribution in units of counts while the right vertical axis is cumulative distribution in %.

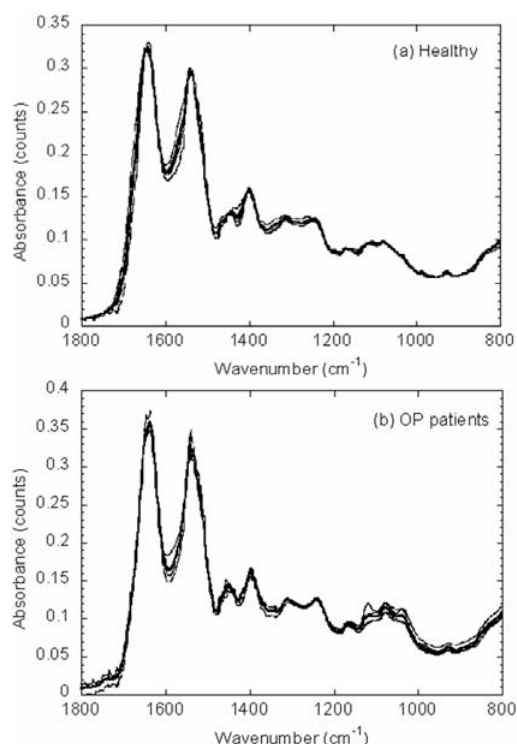


Fig. 2. Trends of individual sample spectra compared with the average spectra (a) Healthy persons and (b) Patients.

compares it for the grating, to a diode array detector.

The solvents for these determinations are often water for water soluble compounds, or ethanol for organic-soluble com-

pounds. Since human blood or plasma is water soluble, the plasma samples in this study are 100 times diluted by mixing 30 μ l of plasma sample in 3 ml of de-ionized water. All spectroscopic measurements were made in the wavelength range of 250 to 500 nm on the double beam UV/Visible spectrophotometer [21]. Spectral optical densities out of 50 separate measurements are averaged for a sample. The solvent effect on the background level is removed by subtracting the spectral density of pure DI water.

2.4 BMD measurements

BMD measurement, as the state-of-the-art clinical measure of bone integrity, are performed by BMD-DEXA to determine fracture risk of specific bones of the OP patients such as spine, hip and wrist [21]. The density of these bones is then compared with the bone density value averaged over groups at a variety of ages, sexes and heights. The comparison is typically scored by two measures, the T-score and the Z-score [27] which are used to determine fractures risk and the stage of osteoporosis progress in an individual:

$$\text{T-Score} = \frac{\text{subject's BMD value} - \text{mean young normal BMD value}}{\text{young normal BMD standard deviation}}$$

$$\text{Z-Score} = \frac{\text{subject's BMD value} - \text{mean age-matched BMD value}}{\text{age-matched BMD standard deviation}}$$

Hence the osteoporosis is diagnosed when the T-score is smaller than -2.5, representing the BMD of the potential patient lies outside the safe zone (refer to Table 1). The present BMD measurements are made at the total hip bones consisting of lumbar spine (anteroposterior, L1-L4), the femoral neck, trochanteric and intertrochanteric region, with dual energy X-ray absorptiometry (DXA), consisting of lumbar spine (anteroposterior, L1-L4), the femoral neck, trochanteric and intertrochanteric region, with DXA.

3. Results and discussion

3.1 Physical parameters of the plasma samples

The physical parameters, i.e., hydrodynamic size and pH are measured to ensure for the plasma samples to be in similar colloidal state, because the parameters are key factors determining the stability of the colloids and any change in the parameters during the optical measurement can generate transient artifacts in the results [22]. The results of the plasma samples were verified with the help of Zeta Potential (Otsuka, co., Japan, OTSUKA ELS-8000). The sample is 50 times diluted with DI water and the hydrodynamic size of proteins in the sample is then measured by the dynamic light scattering (DLS, Otsuka co., Japan, ELS-8000). From ten measurements on each sample, we verify that the plasma proteins are in the range of 15 to 20 nm as seen in Fig. 1 and the size is kept nearly constant. The pH of the samples was also measured using a pH meter (Thermo Orion, 410) with the

typical error of 0.2 pH. The averaged pH value of the plasma samples was found to be 7.4.

3.2 Spectral analysis

Fig. 2 shows typical examples of the FTIR spectra for 5 samples of healthy persons and 5 samples of patients. Single narrow lines in Fig. 2 correspond to the averaged spectra of 5 individual measurements for each person, while the bold line represents the overall averaged result of all persons. The figure shows the good reproducibility in terms of both intensity and peak position of the spectrum. On the basis of the Beer-Lambert law, absorbencies of molecules regarding the organic matter within the plasma help to identify the molecular groups. The spectra are dominated by two absorbance peaks at 1646 and 1540 cm^{-1} , corresponding to the amide I and amide II bands, respectively. While the amide I arises from C=O stretching, amide II group arises from N-H bonds or C-N stretching or CNH bending vibrations [1, 17]. Similarly, the absorbance at 1480 - 1432 cm^{-1} is mainly due to CH_2^- and CH_3^- stretching vibrations from the lipids and proteins. Existence of Amide III band at 1270 cm^{-1} which arises from coupling of C-N stretching and N-H bending indicates existence of some proteins consisting of C, N and H. The bands at 900–1300 cm^{-1} are assigned to C-O bending modes of saccharides (glucose, lactose and glycerol), the peaks at 1360–1430 cm^{-1} are attributed to COO^- of amino acids, and the peak at 1430–1480 cm^{-1} is attributed to fatty acids, phospholipids and triglycerides [19-24].

The aforementioned assignments of molecular constituents are consistent well with literature reports of Delerisa and Petiboisa [24] for the Amide I; Petibios et al. [25] for Amide II and secondary groups. Those are summarized in Table 2 [17, 18, 24-26]. Even though the overall trends of the spectra are not varied much as seen in Fig. 2(a) and (b), the intensities of some peaks from the OP patient's samples are rather discriminated from those from the normal sample in the statistical point of view, together with slight change in intensity.

Analysis of the FTIR spectrum has been made for the better interpretation of results of constituents of plasma in a quantitative manner. The intensity of the amide bands of normal plasma samples were about 10 % lower than those in patient's sample. The amplitude of the spectra was found to be differed as seen in Fig. 3 and the differences in the amplitude are statistically meaningful as shown in Figs. 3-6. The FTIR spectra obtained are analyzed for various peaks at different wavenumbers to indicate a quantitative analysis for each peak of interest. The peak deconvolution is made consistently to produce quantitative analysis of the sub peaks and the fitted line is matched well with the experimental data.

Fig. 4 shows that the two major peaks representing amide I and II groups as seen in Fig. 3 are deconvoluted by Gaussian profiles the fittings of which are all in good agreements with the experimental data lines. As a result, the two peaks are composed of 5 sub peaks. The peaks at 1646 cm^{-1} and 1540

Table 2. Range of major components of Blood plasma.

Range (cm^{-1})	Major components
1739-1732	ν (C=O): lipids, cholesterol esters, triglycerides
1720-1600	ν (C=O): (amide-I) β -sheet: proteins, turns, coils.
1630-1560	δ (NH_2): amino acids
1600-1480	δ (N-H): (amide II) alpha-helix: proteins
1480-1430	δ_{as} (CH_3), δ_{as} (CH_2), δ_{as} (CH_2): fatty acids, phospholipids, triglycerides, ν (COO^-): amino acids
1430-1360	ν (C-O): saccharides, glucose, lactate, glycerol
1300-900	C-N stretch: aliphatic ammine
1150-1000	N-H bending of amine salt
850-750	Broad absorption by NH_2 wag in aliphatic amines
800-600	Aliphatic primary or secondary amides
750-700	Fingerprint region

ν : stretching vibrations, δ : bending (scissoring) vibrations, as: asymmetric [24].

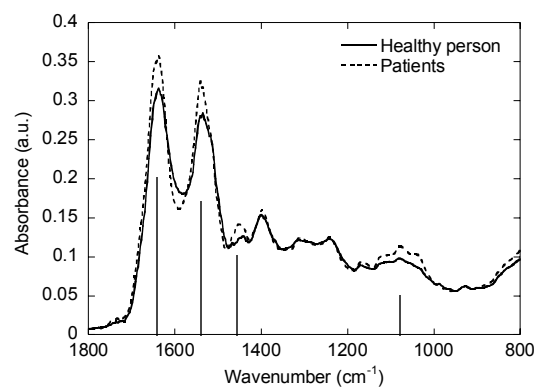


Fig. 3. Comparison of the spectra of healthy and OP patient plasma samples.

cm^{-1} , attributed to the amide groups, increase in intensity for patients group. On the other hand, the valley between the peaks is supported by a new hidden peak at 1588 cm^{-1} which is clearly attributed to the amino acid group (NH_2). The peak is lower for the patient's plasma as compared to the healthy person's plasma.

Fig. 5(a) shows that spectral absorbencies of patient samples are always significantly higher than those of healthy sample in the wavenumber range of 1420 – 1480 cm^{-1} . Regarding the pre-mentioned good repeatability of the measurements (see Fig. 2), the increase in intensity for patient group lies above uncertainty range. Similar deconvolution process is applied to the spectra in Fig. 5(a) after baseline correction (not shown here).

As a result, Fig. 5(b) shows that the spectra for both groups consist of three subpeaks, among which we would note that the biggest difference is generated at 1456 cm^{-1} and also much higher than any changes in Fig. 4 as well. The dissimilarity of peak intensity at 1456 cm^{-1} for both groups might be considered as a new promising biomarker for the OP early diagnosis.

Thus, we focus on the highest sub-peak at 1456 cm^{-1} which is attributed to the CH_2/CH_3 appearing from the vibrations of

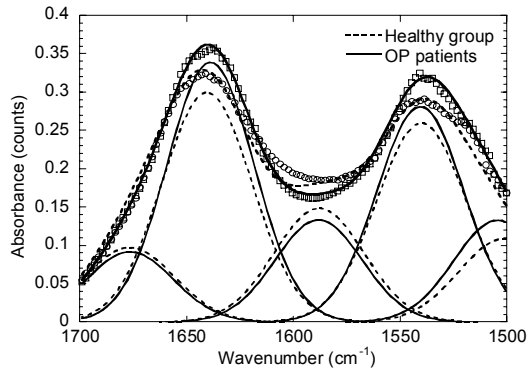


Fig. 4. Identifying the special peak at 1600 cm⁻¹ using deconvolution for healthy and patients spectra. Symbols such as circle and square represent experimental data.

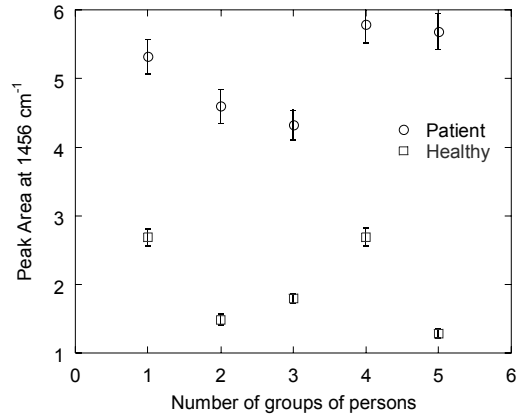


Fig. 6. Statistical analysis of healthy and patient’s spectra for 1456 cm⁻¹ peak.

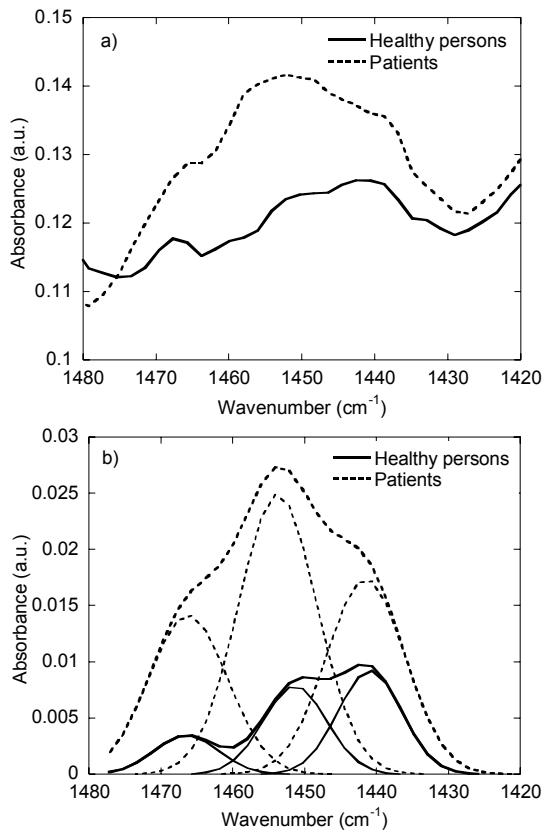


Fig. 5. (a) Identifying the special peak at 1456 cm⁻¹ using deconvolution into three subpeaks and (b) Peak area of 1456 cm⁻¹.

lipids and proteins. It is notable that the subpeak area obtained from the peak analysis would represent the relative concentration of the corresponding bio-molecules better than the peak intensity. Fig. 6 shows that the peak area from the patients is always two times larger than that from the healthy persons within the present investigated groups. The peak at 1077 cm⁻¹ has been more prominently seen to be increasing for all patients’ plasma in comparison to the healthy person’s sample. This peak is attributed to the C-N stretch, aliphatic ammine group, which seems to appear in blood plasma due to the disrupted α helix of the collagen chain. In the deconvoluted spec-

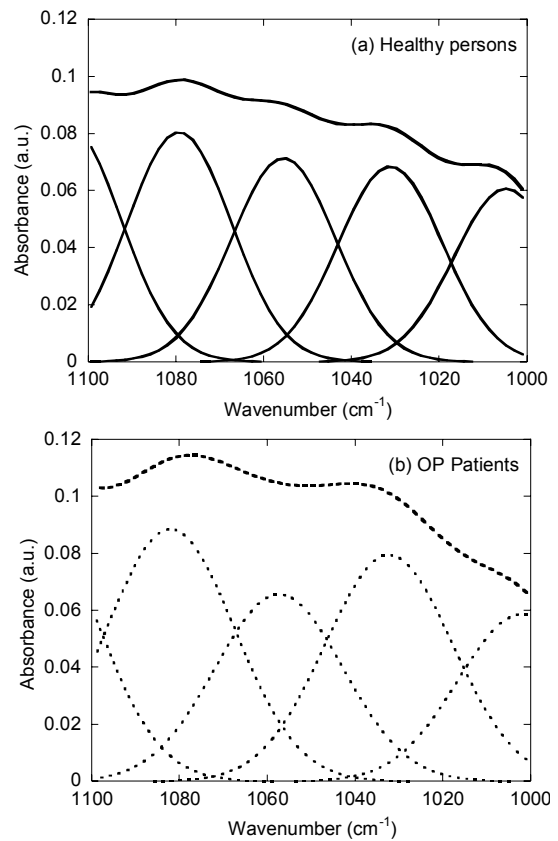


Fig. 7. Identifying special peaks of the FTIR spectra of plasma normal samples and OP patient for 1040 cm⁻¹.

tra, the patient’s plasma shows 0.08 count higher in intensity than healthy person’s plasma does as compared in Figs. 7(a) and (b), respectively.

Thus, according to the analysis, the observations are very likely to indicate a general difference in the plasma metabolites of the Osteoporotic patients, especially in terms of three unique peaks at 1588, 1456 and 1077 cm⁻¹. These remarkable changes have occurred due to the increased absorption of the released proteins from bone. More degradation of the osteo-

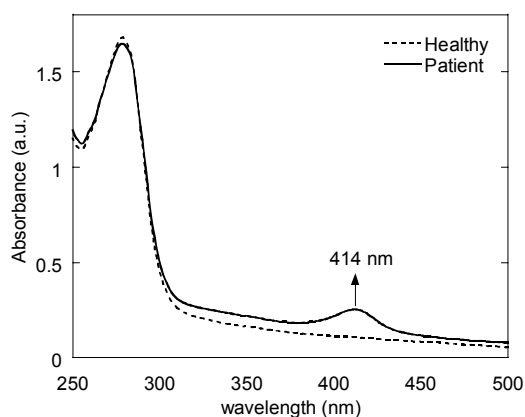


Fig. 8. UV-visible spectroscopy results for healthy and patient are blood plasma.

clast [12] releases more amount of the bonemarkers, which are the degraded products of the type I collagen, according to the theory of bone modeling and the degradation of bone by Raisz (1997) [27]. The collagen helices structure is generally stabilized by the bonds of $(CH_2)_2-CH_2$ or C-H groups, N-H and NH_2 . Hence it might be the degraded product of the collagen protein which appears to be higher in OP patients, due to the imbalance in the bone metabolism.

The UV/Visible spectra of the healthy and patient's plasma also shows good repeatability in the experimental data. For better comparison, averaged spectra for both groups are compared in Fig. 8. Interestingly, new and unique peaks are appeared at 279 nm and 414 nm only in the patient sample spectra. This verifies that some molecules absorbing 414 nm light exist only in the patient samples.

As discussed above, the FTIR intensity of the two peaks at 1456 and 1033 cm^{-1} is higher for patient plasma as compared with healthy persons' plasma. Therefore, the new appearance of the 414 nm and 279 nm peak seems to support again our previous inference about the release of the bonemarkers from the FTIR measurements.

3.3 Cluster analysis

Clustering is the classification of objects into different groups, giving the proximity, according to some defined distance measure [1, 25, 28]. A hierarchical algorithm is used to investigate and quantify the mutual relevance between successive clusters in terms of heterogeneity values [18]. The distance measured determines the similarity of two elements. The whole spectra and/or a limited range of the spectra are classified on every investigated member, so as to find the most homogeneous groups between spectra. Each group is identified with the smallest growth in heterogeneity, i.e. the geometric distance in the tree structure. The heterogeneity values between groups of spectra, proportional to their absorption differences [18].

Cluster analysis performed by using the SPSS software with standard making distance matrix and ward's algorithm dendro-

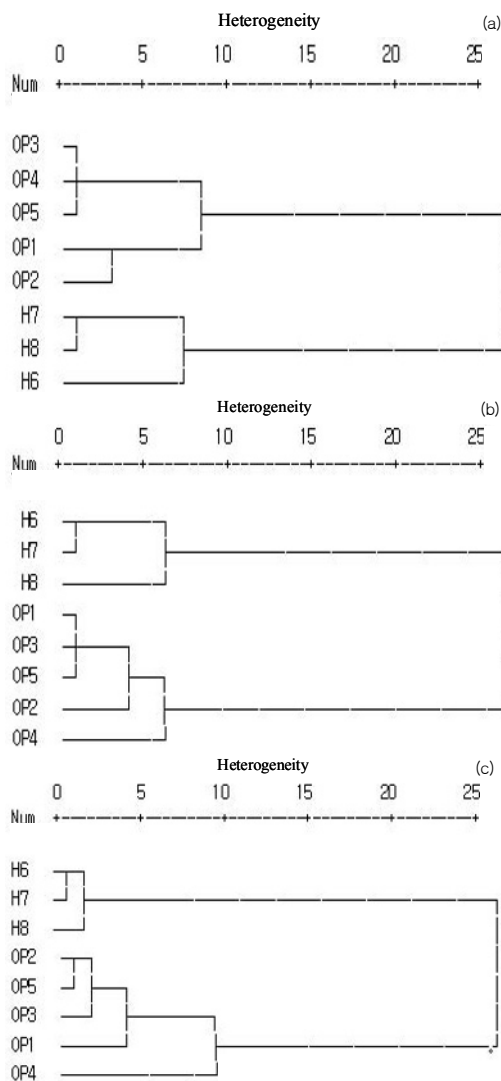


Fig. 9. Cluster analysis of the IR spectra examined for healthy and patient samples in different peak regions (a) around 1456 cm^{-1} , (b) at $1637\text{--}1639\text{ cm}^{-1}$, (c) at $1539\text{--}1541\text{ cm}^{-1}$ (where H represents groups of Healthy & OP represents the group of patients).

gram. The spectra classification has been performed here independently for each population on complete spectra. The entire spectrum from 600 to 2000 does not completely succeed to distinguish between healthy and OP patient groups (some groups does not fit with the patients groups). However each subset region in the vicinity of the peaks gives good classification at $1637\text{--}1648$, $1539\text{--}1542\text{ cm}^{-1}$ as shown in Fig. 9. The spectra at 1456 cm^{-1} is most specific for CH_2/CH_3 groups, appearing from lipids and proteins, with high heterogeneity between the healthy and OP patients group. The classification, made for 1637 to 1648 cm^{-1} absorption region, revealed the heterogeneity values highly correlated with observed amide I within the population. Fig. 9 (c) represents the classification with the spectra at $1539\text{--}1542\text{ cm}^{-1}$. This gives clear distinction between the patients and healthy groups for the amide II group.

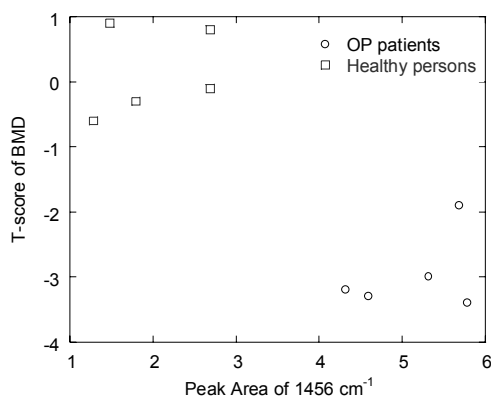


Fig. 10. BMD correlation with peak area of 1456 cm⁻¹.

3.4 BMD analysis

Since there have been found prominent spectral and statistical differences from the optical measurements, they are considered as possible bone biomarkers. Hence it is important to confirm the potential patients warned by the optical detection with the clinical test by BMD score measurement. For this reason, the BMD measurements were carried out with the same samples for both groups. It was found that the T-scores of the potential patients are sufficiently low. Table 2 summarizes that the T-scores from the patients are almost in the range of osteoporosis (<-2.5) with the minimum of -3.0 and the maximum of -4.0 except one patient, -1.9. We tried to correlate our data with the T-score, leading the score to having an inverse relationship with the peak area. Even though the data in the correlation are somewhat scattered in Fig. 10, the peak at 1456 cm⁻¹ is quite useful to separate the OP patients from the tested groups. The scatter of the data would be related to the feature of the BMD measurement: the BMD is a static measure of bone calcium content and does not reflect the current metabolic activity of bone [27].

4. Conclusions

A novel approach based on the detection of blood plasma constituents with FTIR (Fourier Transform Infrared Spectroscopy) and UV/Visible spectroscopy has been utilized. The results obtained are useful for reliable indication of the presence of the osteoporosis in the patients, and will assist in the early diagnosis of the disease. New peaks at 1646, 1540, 1588, 1077 and 1456 cm⁻¹ in the FTIR spectra are indicative of the presence of N-H stretch, CH₂/CH₃ and NH₂ groups respectively and can be used as biomarkers for the future diagnosis. Similarly a unique peak has been identified for 414 nm wavelength for osteoporosis patient. The BMD T-score results showed the inverse relation with the optical spectra intensity and gave verification for potential patients. These results could be considered as preliminary results for further investigation. The interesting and consistent spectral differences between patient and healthy spectra may be considered as a promising

basis for a future study including large number of samples.

Acknowledgment

K. Singh is thankful to the Korean Research Foundation for their support funded by Korean Government (KRF-2005-211-D00203), to Indira Gandhi National Open University, New Delhi, India and KHAN Company, Korea for the encouragement. This study has been supported by a grant of the Korea Health 21 R&D Project (02-DJ3-PG6-EU05-0001), Ministry of Health & Welfare, Republic of Korea and also supported by Korea Research Foundation Grant funded by Korean Government (MOEHRD) (Project No. R08-2003-000-10858-0).

References

- [1] M. Huleihela, M. Karpasasb, Y. S. Talyshanskyb, Y. Doubijanskib and V. Erukhimovitchb, Mass spectroscopic and IR spectroscopic evaluation of abnormal biological samples, *Vacuum*, 78 (2005) 557-562.
- [2] C. L. Deal, Osteoporosis: prevention, diagnosis, and management, *Am. J. Med.*, 102 (1A) (1997) 35S-39S.
- [3] J. D. Currey, Bone strength: what are we trying to measure?, *Calcif. Tissue Int.*, 68 (2001) 205-210.
- [4] K. Singh, K. S. H. Lee and K. C. Kim, Review: Osteoporosis: New Biomedical Engineering Aspects, *J. Mech. Eng. Sci. Technol.*, 20 (2006) 2265-2283.
- [5] S. Phillips, N. Fox, J. Jacobs and W. Wright, The direct medical costs of osteoporosis for American women aged 45 and older, *Bone*, 9 (1986) 271.
- [6] N. McCarroll, Bone Disorders (Osteoporosis), *Anal. Chem.*, 65 (1993) 388-395.
- [7] M. Demers, Clinical usefulness of markers of bone degradation and formation, *Scand. J. Clin. Lab. Invest.*, 227 (1997) 12-20.
- [8] D. Chen, N. V. Sarikaya, H. Gunn, S. W. Martin, and J. D. Young, ELISA methodology for detection of modified osteoprotegerin in clinical studies, *Clin. Chem.*, 47 (2001) 747-749.
- [9] H. U. Gremlich, The use of optical spectroscopy in combinatorial chemistry, *Biotech. Bioeng.*, 61 (1998) 179-187.
- [10] J. B. Lesh, K. Schultz and J. D. Porsche, Fractionation of Blood Plasma, *Ind. Eng. Chem.*, 42 (1950) 1376-1380.
- [11] D. Naumann, H. Helm and H. Labischinski, Microbiological Characterizations by FT/IR Spectroscopy, *Nature*, 351 (1991) 81-82.
- [12] W. Boyle, W. S. Simonet and D. L. Lacey, Osteoclast differentiation and activation, *Nature*, 423 (2003) 337-342.
- [13] X. H. Luo, L. J. Guo, P. F. Shan, H. Xie, X. P. Wu, H. Zhang, X. Z. Cao, L. Q. Yuan and E. Y. Liao, Relationship of circulating MMP-2, MMP-1, and TIMP-1 levels with bone biochemical markers and bone mineral density in postmenopausal Chinese women, *Osteoporos. Int.*, 17 (2006) 521-526.
- [14] P. R. Griffiths and de J. A. Haseth, *Fourier Transform*

- Infrared Spectrometry*, John Wiley & Sons, New York (1986).
- [15] K. K. Chittur, FTIR/ATR for protein adsorption to biomaterial surfaces, *Biomaterials*, 19 (1998) 357-369.
- [16] D. Naumann, Infrared Spectroscopy in Microbiology, in *Encyclopedia of Analytical Chemistry*, R.A. Meyers, Ed.; John Wiley & Sons, New York, (2000) 102-131.
- [17] D. Y. Tseng, R. Vir, S. J. Traina and J. J. Chalmers, A Fourier-Transform Infrared spectroscopy analysis of organic material degradation in a bench-scale solid substrate fermentation (composting) system, *Biotech. Bioeng.*, 50 (1996) 661-670.
- [18] V. Erukhimovitch, M. Talyshinsky, Y. Souprun and M. Huleihel, FTIR spectroscopy examination of leukemia patient's plasma, *Vib. Spectrosc.*, 40 (2006) 40-46.
- [19] V. Erukhimovitch, M. Talyshinsky, Y. Souprun and M. Huleihel, Use of Fourier Transform infrared microscopy for evaluation of drug efficiency, *J. Biomed. Opt.*, 11 (2006) 640009.
- [20] R. A. Shaw, S. Kotowich, M. Leroux and H. H. Mantsch, Multianalyte serum analysis using mid-infrared spectroscopy, *Ann. Clin. Biochem.*, 35 (1998) 624-632.
- [21] A. Nanoyama, *Using multiwavelength UV-Visible spectroscopy for the characterization of red blood cells: An investigation of Hypochromism*, Ph.D Thesis, Univ. of Florida (2004).
- [22] D. Lee, J.-W. Kim and B. G. Kim, A New Parameter to Control Heat Transport in Nanofluids: Surface Charge State of the Particle in Suspension, *J. Phys. Chem. B*, 110 (2006) 4323-4328.
- [23] P. D. Delmas, R. Eastell, P. Garnero, M. J. Seibel and J. Stephan, The use of biochemical markers of bone turnover in osteoporosis, *Osteoporos. Int.*, 11 (2000) S2-S17.
- [24] G. De'le'risa and C. Petiboisa, Applications of FT-IR spectrometry to plasma contents analysis and monitoring, *Vib. Spectrosc.*, 32 (2003) 129-136.
- [25] C. Petibios, G. Cazorla, H. Gin and G. Deleris, Differentiation of populations with different physiologic profiles by plasma Fourier-transform infrared spectra classification, *J. Lab. Clin. Med.*, 137 (2001) 184-190.
- [26] R. J. H. Clark and R. E. Hester, *Biomedical applications of spectroscopy*, Wiley & Sons, 1st ed., New York (1996).
- [27] L. G. Raisz, The osteoporosis revolution, *Ann. Intern. Med.*, 126 (1997) 458-462.
- [28] P. Lasch, W. Haensch and D. Naumann, M. Diem, Imaging of colorectal adenocarcinoma using FT-IR microspectroscopy and cluster analysis, *Biochim. Biophys. Acta*, 1688 (2004) 176-186.



Kanika Singh was awarded her PhD (MEMS-Nano), Pusan National Univ, Korea, 2008, M.Tech (Electr Instr Tech), IIT-Delhi, & University of Karlsruhe, Germany, 2002. She has over 40 research papers in journals/conf Proc. She was an awardee of 'IEEE Out-standing Young Engineer Award (India)', 'Outstanding Paper Awards: (Japan; Postech-Korea) and 'IEEE-EMBS Best Student Paper Award (USA). She is now a Manager/ Sr. Engineer (E & I) in KHAN Company, Korea and co-assigned as an Asst. Professor (Electrical Eng) in Indira Gandhi National Open Univ, India. Her areas of interest are Nano-Micro Sensors, Electrical Instrumentation and Biomedical Engineering.



Donggeun Lee is an associate professor at School of Mechanical Engineering, Pusan National University and is now leading a research group on development of nanoparticle-related energy components. More information is available in <http://home.pusan.ac.kr/~mnht>.



Kyung Chun Kim received a B.S. in Mechanical Design Engineering from Pusan National University in 1979, then received his M.S. and Ph.D. in Mechanical Engineering from KAIST in 1981 & 1987, respectively. He is now a professor at the School of Mechanical Engineering at Pusan National University.